Robust Motion and Correspondence of Noisy 3-D Point Sets with Missing Data

Emanuele Trucco [a], Andrea Fusiello [b], Vito Roberto [b]

[a] *Department of Computing and Electrical Engineering*
Heriot-Watt University, Edinburgh, UK

[b] *Laboratorio Immagini, Dipartimento di Matematica e Informatica*
Università di Udine, Udine, IT

Abstract

We describe RICP, a robust algorithm for registering and finding correspondences in sets of 3-D points with significant percentages of missing data, and therefore useful for both motion analysis and reverse engineering. RICP exploits LMedS robust estimation to withstand the effect of outliers. Our extensive experimental comparison of RICP with ICP shows RICP's superior robustness and reliability.

Key words: ICP, Registration, CAD-based Vision, Motion Estimation, Reverse Engineering

1 Introduction

This paper addresses the registration of noisy sets of 3-D points, a percentage of which is present in one set but not in the other, and in the absence of correspondence information. This problem has been considered mainly in two applicative domains, *motion analysis* and *reverse engineering*. Apart from the differences in emphasis discussed below, algorithms from both domains solve basically the same two problems: estimating the 3-D motion (rotation matrix

and translation vector) aligning the two sets of points, and establishing a correspondence between points. The two problems are intimately connected; (Wang et al., 1996) gives a nice illustration of their mathematical symmetry.

Motion estimation (Goldgof et al., 1992; Ito and Aloimonos, 1988; Lee and Joshi, 1993; Wang et al., 1996) aims to compute the motion aligning the point sets. Points are typically extracted by passive ranging systems such as feature-based stereo. Least-squares (LS) solutions are well-known for the *ideal motion problem* (both sets contain the same number of points affected by moderate sensor noise (Kanatani, 1993)), but fail for the *general motion problem*, whereby several points, called *outliers*, have no correspondence in the other set and may lie far from matched points. (Wang et al., 1996) is representative of recent work in this area. The authors propose an efficient, heuristic outlier removal scheme, cast as a solution of a graph assignment problem. Motion is estimated after correspondence is established. However, the speed advantages are limited by several factors: the method depends on a heuristic threshold, is ostensibly sensitive to even moderate Gaussian noise, and can cope with only limited percentages of outliers.

Reverse engineering aims to acquire an accurate, complete surface model of a 3-D object from several range views (Chen and Medioni, 1992; Eggert et al., 1996; Stoddart et al., 1998). Dense data points (e.g., tens of thousands of triangulated points per view) are typically acquired by active ranging systems like laser scanners (Trucco et al., 1998). Sensor noise from state-of-the-art laser scanners is low (around one part in one thousand). Most algorithms in this domain are variations of the *Iterative Closest Point* algorithm (ICP) introduced in (Besl and McKay, 1992). ICP can give very accurate results for densely sampled surfaces, but results deteriorate with outliers, created at least by non-overlapping areas between views. In this case, the overlapping surface portions must start very close to each other to ensure convergence, making the initial position a critical parameter. (Bispo and Fisher, 1996; Brujic and Ristic, 1996) report quantitative studies of ICP performance. The most relevant

findings for our purposes are that (i) the initial registration guess affects only the speed of convergence (not registration accuracy), as long as it is chosen within the convergence basin of the target minimum; (ii) accurate registration is possible with no outliers, and requires very accurate measurements and high numbers of points; (iii) acceptable accuracy (for reverse engineering) can be achieved with 2-300 points.

This paper introduces RICP, an algorithm for registering robustly a limited number of sparse 3-D points (say about 100) corrupted by significant percentages of outliers. Robustness is achieved thanks to the Least Median of Squares (LMedS) regression (Rousseeuw and Leroy, 1987), which has been used successfully in many areas on computer vision (Meer et al., 1991; Torr and Murray, 1997). (Masuda and Yokoya, 1995) also report a robust registration method based on ICP and LMedS. Their method iterates a 3-step sequence of processes: random sampling, estimation of the motion parameters with ICP, and evaluation. The sequence *as a whole* makes up the LMedS algorithm. On the contrary, in our approach, LMedS (with random sampling) is used *inside* the ICP, where it replaces the LS rotation estimation. This enables us to use a dynamic translation estimate based on outlier-free data in the ICP iteration. Moreover, as shown by our experiments, RICP achieves a larger basin of attraction and more accurate registrations than ICP.

RICP is interesting for both correspondenceless motion, in which sets of sparse points are frequently used, and free-form surface matching, as outliers occur inevitably when multiple views are acquired. In the latter case, RICP can both produce initial alignments and find outliers in subsampled surface data. As it acts on sparse point sets, RICP performs a neighbour search on a set of points rather then finding the closest point (CP) on a true surface. This is similar to some ICP variations (Blais and Levine, 1995; Zhang, 1994) in which dense surface data are sampled uniformly to achieve a sparse set of control points used for registration. Notice that RICP still works with dense data, but the advantages over ICP are smaller unless many outliers are present.

In the following, Section 2 summarises ICP and its main features, Section 3 presents RICP, Section 4 reports our experimental evaluation of RICP, and Section 5 discusses RICP's contributions and limitations.

2 A brief summary of ICP

This section summarizes ICP and some features of our ICP implementation. Let $\mathcal{P} = \{\mathbf{p}_i\}_1^{N_p}$ and $\mathcal{M} = \{\mathbf{m}_i\}_1^{N_m}$ the two sets of 3-D points to align, which we call respectively *data* and *model*. In general, $N_p \neq N_m$. The problem is to compute the rotation $\mathbf{R}$ and translation $\mathbf{t}$ producing the best alignment of $\mathcal{P}$ and $\mathcal{M}$:

$$\mathcal{M} = \mathbf{R}\mathcal{P} + \mathbf{t}, \tag{1}$$

meaning that $\mathbf{R}$ and $\mathbf{t}$ are applied to each point in the set $\mathcal{P}$. In general, this equation will not be satisfied exactly by all points, hence the equality should be interpreted in the least square sense.

Let us define the *closest point* in the model to a data point $\mathbf{p}$ as

$$\mathrm{cp}(\mathbf{p}) = \arg\min_{\mathbf{m}\in\mathcal{M}} \|\mathbf{m} - \mathbf{p}\|.$$

We can then summarize ICP as follows:

1. Compute the subset of CPs: $\mathcal{Y} = \{\mathbf{m} \in \mathcal{M} \mid \mathbf{p} \in \mathcal{P} : \mathbf{m} = \mathrm{cp}(\mathbf{p})\}$;

2. Compute a LS estimate of the motion bringing $\mathcal{P}$ onto $\mathcal{Y}$:

$$(\mathbf{R}, \mathbf{t}) = \arg\min_{\mathbf{R},\mathbf{t}} \sum_{i=1}^{N_p} \|\mathbf{y}_i - \mathbf{R}\,\mathbf{p}_i - \mathbf{t}\|^2. \tag{2}$$

where $\mathbf{y}_i \in \mathcal{Y}$ and $\mathbf{p}_i \in \mathcal{P}$.

3. Apply the motion to the data points:

$$\mathcal{P} \leftarrow \mathbf{R}\mathcal{P} + \mathbf{t}.$$

4. If the stopping criterion (see below) is satisfied, exit; else go to **1.**

The algorithm stops as soon as one of the following conditions is satisfied:

- the mean square error (MSE) $d = 1/N_p \sum_{i=1}^{N_p} ||\mathbf{y}_i - \mathbf{p}_i||^2$ is sufficiently small;
- the MSE difference between two successive iterations is sufficiently small;
- the maximum allowed number of iterations has been reached.

It has been proven (Besl and McKay, 1992) that ICP converges monotonically to a local minimum of the MSE, an index commonly used along with its derivative with respect to the step index (Besl and McKay, 1992; Bispo and Fisher, 1996; Stoddart et al., 1998; Zhang, 1994).

For step **1**, we have implemented CP algorithms based on exhaustive search (acceptable with small point sets) and k-D trees (Besl and McKay, 1992; Zhang, 1994).

In step **2**, motion parameters are computed using a technique involving the SVD, which has been shown to yield the best global accuracy and stability (Lorusso et al., 1997). Since (1) is satisfied by the centroids of the point sets as well, we can eliminate translation by defining the *centralized* sets:

$$\mathbf{p}_{c,i} = \mathbf{p}_i - \bar{\mathbf{p}} \quad \text{and} \quad \mathbf{y}_{c,i} = \mathbf{y}_i - \bar{\mathbf{y}}$$

where

$$\bar{\mathbf{p}} = 1/N_p \sum_{i=1}^{N_p} \mathbf{p}_i \quad \bar{\mathbf{y}} = 1/N_p \sum_{i=1}^{N_p} \mathrm{cp}(\mathbf{p}_i).$$

Note that we estimate centroids $\bar{\mathbf{p}}$ (data) and $\bar{\mathbf{y}}$ (model) *at each iteration*, using only the N_p points that are CP for at least one data point, hence a model point increases its weight in the computation if it is the CP of several data points.

Problem (2) is then equivalent to the following problem:

$$\min_{\mathbf{R}} \sum_{i=1}^{N_p} ||\mathbf{y}_{c,i} - \mathbf{R}\mathbf{p}_{c,i}||^2, \quad \text{(with } \mathbf{R} \text{ rotation matrix)} \tag{3}$$

that is minimized when trace($\mathbf{RK}$) is maximized (Kanatani, 1993), where

$$\mathbf{K} = \sum_{i=1}^{N_p} \mathbf{y}_{c,i} \mathbf{p}_{c,i}^{\top}.$$

If the SVD of $\mathbf{K}$ is given by $\mathbf{K} = \mathbf{VDU}^{\top}$, then the optimal rotation matrix that maximizes the trace is $\mathbf{R} = \mathbf{VU}^{\top}$. The optimal translation is then computed as $\mathbf{t} = \bar{\mathbf{y}} - \mathbf{R}\bar{\mathbf{p}}$.

Extensive experimentation with our ICP implementation confirmed ICP's good performance with full overlap (all points in both views) and initial motion guesses very close to the solution, and its sensitivity to outliers (e.g., partial overlap) (Bispo and Fisher, 1996; Brujic and Ristic, 1996). Outliers skew the distribution of the residuals $r_i = ||\mathbf{y}_i - (\mathbf{R}\mathbf{p}_i + \mathbf{t})||$, and consequently LS motion estimates. In addition, outliers skew the centroid estimate, and consequently rotation estimates obtained after shifting data points to the centroid (Kanatani, 1993).

3 RICP: a Robust ICP algorithm

This section outlines RICP, our robust algorithm for correspondenceless point matching. Problem and notation are the same as in Section 2. RICP replaces step **2** of ICP with a robust estimation of motion, based on LMedS.

The principle behind LMedS is the following: given a regression problem, where the number of parameters is d, compute a candidate model based on a randomly chosen d-tuple from the data; estimate the fit of this model to *all* the data, defined as the median of the squared residuals, and repeat optimizing the fit. The data points that do not belong to the optimal model, which represent the majority of the data, are *outliers*. The *breakdown point*, i.e., the smallest fraction of outliers that can yield arbitrary estimate values, is 50%. In principle all the d-tuples should be evaluated; in practice a Monte Carlo technique is applied, in which only a random sample of them of size m is con-

sidered. Assuming that the whole set of points may contain up to a fraction ϵ of outliers, the probability that at least one of the m d-tuple consist of d inliers is given by

$$P = 1 - (1 - (1 - \epsilon)^d)^m. \tag{4}$$

Hence, given d, ϵ, and the required P (close to 1), one can determine m:

$$m = \frac{\log(1 - P)}{\log(1 - (1 - \epsilon)^d)}. \tag{5}$$

When Gaussian noise is present in addition to outliers, the relative statistical efficiency (i.e., the ratio between the lowest achievable variance for the estimated parameters and the actual variance) of the LMedS is low; to increase the efficiency, it is advisable to run a weighted LS fit after LMedS, with weights depending on the residual of the LMedS procedure (Rousseeuw and Leroy, 1987).

In order to use LMedS for computing rigid motion in (step **2**), we release temporarily the constraint of $\mathbf{R}$ being a rotation matrix, and we cast the problem of computing the matrix $\mathbf{R}$ as a linear regression problem with nine parameters (the entries of $\mathbf{R}$ are considered independent).

Estimating rotation. As in the previous case, we first eliminate translation by shifting data and model in the centroid (see next paragraph), thereby obtaining:

$$\left[\mathbf{y}_{c,1} \dots \mathbf{y}_{c,N_p}\right] = \mathbf{R}\left[\mathbf{p}_{c,1} \dots \mathbf{p}_{c,N_p}\right]$$

which can be re-written as an over-constrained system of linear equations:

$$\mathbf{L}\mathbf{r} = \mathbf{b} \tag{6}$$

where $\mathbf{L}$ is a $3N_p \times 9$ matrix given by

$$\mathbf{L} = \begin{bmatrix} \begin{bmatrix} \mathbf{p}_{c,1}^\top \\ \dots \\ \mathbf{p}_{c,N_p}^\top \end{bmatrix} & \mathbf{0} & \mathbf{0} \\ \mathbf{0} & \begin{bmatrix} \mathbf{p}_{c,1}^\top \\ \dots \\ \mathbf{p}_{c,N_p}^\top \end{bmatrix} & \mathbf{0} \\ \mathbf{0} & \mathbf{0} & \begin{bmatrix} \mathbf{p}_{c,1}^\top \\ \dots \\ \mathbf{p}_{c,N_p}^\top \end{bmatrix} \end{bmatrix}, \tag{7}$$

$\mathbf{r}$ (9×1) is obtained by juxtaposing the rows of the matrix $\mathbf{R}$, and $\mathbf{b}$ $(3N_p \times 1)$ is obtained by juxtaposing the rows of the matrix $[\mathbf{y}_{c,1} \dots \mathbf{y}_{c,N_p}]$. The unknown vector $\mathbf{r}$ is then computed by solving (6) with the Monte Carlo LMedS method as follows:

(1) select randomly 3 data points, and build a 9×9 system matrix $\mathbf{L}^*$ as in (7);
(2) let $\mathbf{r}^*$ be the solution of the resulting linear system;
(3) compute the residuals of this solution with respect to all the points

$$\mathbf{s} = \mathbf{L}\mathbf{r}^* - \mathbf{b}; \tag{8}$$

(4) repeat from step (1) minimizing the median of the squared residuals, until m samples have been evaluated.

In our implementation we assume $\epsilon = 0.5$, and require $P = 0.95$, thus the size of random sample is $m = 1533$.

The residuals s_j, $j = 1, \ldots, 3N_p$ of (6) are then used to generate the weights for the final, weighted LS regression as follows. First, a robust standard deviation estimate (Rousseeuw and Leroy, 1987) is computed as

$$\hat{\sigma} = 1.4826 \left(1 + \frac{5}{2N_p - d + 1}\right) \sqrt{\underset{j}{\text{med}}\, s_j^2}, \tag{9}$$

where d is the number of parameters (9 in our case). Second, a weight is assigned to each residual, such that

$$w_j = \begin{cases} 1 & \text{if } |s_j| \leq 2.5\hat{\sigma}, \\ 0 & \text{otherwise.} \end{cases}$$

Notice that the w_j are associated to the individual coordinates of 3-D data point $\mathbf{p}_{c,i}$. A weight w_i^* is assigned to each point $\mathbf{p}_{c,i}$, which is zero if at least one of its coordinates has a zero weight, and one otherwise. We therefore deem a point $\mathbf{p}_{c,i}$ an *outlier* if at least one of its coordinates is an outlier*. Finally, we estimate $\mathbf{R}$ by solving (3) with each point weighted by w_i^*. We use SVD to solve the weighted LS problem (similarly to Section 2), which yields a proper rotation matrix.

Estimating centroids. As outliers skew centroid estimates, we adopt a weighted version of the dynamic average (Section 2) taking the average on the outlier-free data: $\bar{\mathbf{p}} = \sum_{i=1}^{N_p} w_i^* \mathbf{p}_i$ and $\bar{\mathbf{m}} = \sum_{i=1}^{N_p} w_i^* \text{cp}(\mathbf{p}_i)$.

4 Experimental results

Synthetic data. A first set of experiments was devoted to compare the accuracy and robustness of RICP and ICP with controlled noise and outliers. We generated model sets of 50 random points each within a unitary

* Equivalently, a point is an outlier if the uniform norm of the point residuals s_i^* is above the threshold $2.5\hat{\sigma}$.

cube (performance depends on shape (Brujic and Ristic, 1996), but a reasonable indication of performance is achieved with non-elongated sets of random points). The data sets were obtained by translating and rotating the models ($\mathbf{t} = (0.2, 0.1, 0.4)^\top$, rotation by 0.17 rad around axis $(1, 1, 1)^\top$; notice the small rotation to guarantee ICP convergence to the correct alignment) and adding Gaussian noise of varying standard deviation. Following (Wang et al., 1996) outliers were simulated by dropping points at random from both sets, but avoiding to drop corresponding pairs from the two sets. For each noise and outlier level, we averaged and recorded the RMS errors, the absolute rotation and translation errors over 50 different realizations of noise and outliers.

Figure 1 shows a typical example of final alignment for ICP and RICP with outliers; the cubes attached to the data emphasize the different quality of the results. Figure 2 summarizes the results, suggesting the better accuracy of RICP. The figure plots the RMS, rotation and translation errors against the intensities of Gaussian noise and outliers (up to 15 points, that is 30% of the data). The rotation and translation errors are the Frobenius norms of the difference between the true and estimated $\mathbf{R}$ and $\mathbf{t}$, respectively. These measures were chosen because (a) they are simple, scalar indices, (b) errors in the direction of the rotation axis (used previously) were artificially high with small rotations, which make axis estimates poorly conditioned, and (c) the RMS error (but not both Frobenius norms of $\mathbf{R}$ and $\mathbf{t}$) may be small for completely wrong alignments with certain shapes. Notice that, with no outliers, the RMS follows the standard deviation of the Gaussian noise, as one expects. Sometimes RICP yields a greater RMS error, because the final weighted LS increase the statistical efficiency of RICP, but it does not reach the efficiency of pure LS, which is optimal with Gaussian noise only. With outliers, the increase of all error indices with the number of outliers is much sharper for ICP than for RICP. The performance degradation of both algorithms seems comparable with 30% outliers (recall that the initial displacement is small to ensure ICP convergence).

We verified the better accuracy of RICP also with different shapes. Figure 3 visualizes an example of final registration with outliers using as model points the corners of a standard calibration jig formed by regular grids of squares arranged on two perpendicular planes. Notice that, unlike the cloud of points above, which spans 3-D volumes, these data are surfaces. Figure 4 shows the results of the same type of tests leading to Figure 2.

In a second set of controlled experiments we verified the larger basin of convergence (the region in $\mathbf{R}, \mathbf{t}$ space guaranteeing convergence to the correct alignment) of RICP with respect to ICP, by observing the RMS and rotation errors (defined as above) for increasingly different initial rotations (from 0 to 180 degrees). We used sets of 30 points within the unitary cube, corrupted by outliers and Gaussian noise as before. Translation was fixed, as we found that rotation has the largest influence on the basin of convergence (because translation is eliminated by centroids subtraction). Figure 5 shows an example of results (with rotation axis $[1, 1, 1]^\top$, 20% outliers, 0.02 noise standard deviation), showing clearly that ICP stops converging before RICP (here, by about 35 degrees) as the initial rotation difference increases. Figure 6 visualizes a case in which ICP does not converge and RICP does, at a parity of initial displacement and noise/outliers conditions.

A final set of experiments proved that RICP leads to more accurate registrations than ICP even with dense data with outliers (partial overlap between views). For instance, Figure 7 shows two range views of a mechanical widget, acquired by a laser scanner, and the registration found by RICP. Figure 8 shows the histograms of the absolute residuals for RICP and ICP, clearly smaller for RICP; the MSE is 7.21 for ICP and 5.01 for RICP.

5 Conclusions

We have presented RICP, a robust, ICP-based algorithm for correspondence-less registration of sparse sets of 3-D points corrupted by sensor noise and outliers. As ICP, RICP does not calculate derivatives or normals, and can be applied to any shape; unlike ICP, it works on sparse point sets, and tolerates substantial amounts of wrong measurements and missing data. With Gaussian noise only, the performances of ICP and RICP are very similar. With outliers, RICP achieves more accurate alignments than ICP (indeed the better the higher the outlier percentage) and converges to the correct registration from a wider range of initial displacements. However RICP has the same applicability of ICP, i.e, finding a precise alignment starting from an approximate one. The issue of finding a rough alignment to start with is not addressed in this paper.

Inevitably, RICP's robustness comes at the cost of a higher complexity. In our tests on a SPARCServer 10 running Solaris 2.5, RICP took, on average, 88 seconds to register synthetic clouds of 50 points with noise and outliers, ICP only half a second. This points strongly to off-line applications for RICP. An intriguing scenario is structure reconstruction from unregistered video sequences acquired by an uncalibrated camera. Consider several, uncalibrated video sequences of the same scene. Usually each sequence spans a continuous range of viewpoints, but the camera jumps discontinuously between sequences. Approximate, point-based Euclidean reconstructions can be computed from each sequence (see (Fusiello, 1998) for a recent review); such 3-D data could be registered by RICP to integrate independent sequences.

Acknowledgement

Thanks to Bob Fisher and Anthony Ashbrooks for the widget data, and to Stefano Morson, Orazio Stangherlin and Gerard Martin for their help. This work

was partially supported by the Italian Space Agency (ASI) under contract ARS-96-185, and by a SOCRATES grant.

References

Besl, P. and McKay, N. (1992). A method for registration of 3-D shapes. *IEEE Transactions on Pattern Analysis and Machine Intelligence*, 14(2):239–256.

Bispo, E. M. and Fisher, R. B. (1996). Free-form surface matching for surface inspection. In Mullineux, G., editor, *The Mathematics of Surfaces VI*, pages 119–136. Clarendon Press, Oxford.

Blais, G. and Levine, M. D. (1995). Registering multiview range data to create 3-d computer objects. *IEEE Transactions on Pattern Analysis and Machine Intelligence*, 17(8):820–824.

Brujic, D. and Ristic, M. (1996). Anaysis of free-form surface registration. In *Proceedings of the IEEE International Conference on Image Processing*, volume II, pages 393–396.

Chen, Y. and Medioni, G. (1992). Object modelling by registration of multiple range images. *Image and Vision Computing*, 10(3):145–155.

Eggert, D. W., Fitzgibbon, A. W., and Fisher, R. B. (1996). Simultaneous registration of multiple range views for use in reverse engineering. In *Proceedings of the International Conference on Pattern Recognition*, pages 243–247, Vienna.

Fusiello, A. (1998). Uncalibrated Euclidean reconstruction: A review. Research Report UDMI/10/98/RR, Dipartimento di Matematica e Informatica, Università di Udine. Submitted for publication in *Image and Vision Computing*.

Goldgof, D. B., Lee, H., and Huang, T. (1992). Matching and motion estimation of three-dimensional point and line sets using eigenstructure without correspondence. *Pattern Recognition*, 25(3):271–286.

Ito, E. and Aloimonos, Y. (1988). Is correspondence necessary for the percep-

tion of structure from motion? In *Proceedings of the Image Understanding Workshop*, pages 921–929.

Kanatani, K. (1993). *Geometric Computation for Machine Vision*. Oxford University Press.

Lee, C. and Joshi, A. (1993). Correspondence problem in image sequence analysis. *Pattern Recognition*, 26:47–61.

Lorusso, A., Eggert, D. W., and Fisher, R. B. (1997). A comparison of four algorithms for estimating 3-d rigid transformations. *Machine Vision and Applications*, 9:272–290.

Masuda, T. and Yokoya, N. (1995). A robust method for registration and segmentation of multiple range images. *Computer Vision and Image Understanding*, 61(3):295–307.

Meer, P., Mintz, D., Kim, D. Y., and Rosenfeld, A. (1991). Robust regression methods in computer vision: a review. *International Journal of Computer Vision*, 6:59–70.

Rousseeuw, P. J. and Leroy, A. M. (1987). *Robust regression & outlier detection*. John Wiley & sons.

Stoddart, A. J., Lemke, S., Hilton, A., and Renn, T. (1998). Estimating pose uncertainty for surface registration. *Image and Vision Computing*, 16:111–120.

Torr, P. H. S. and Murray, D. W. (1997). The developement and comparison of robust methods for estimating the fundamental matrix. *International Journal of Computer Vision*, 24(3):271–300.

Trucco, E., Fisher, R. B., Fitzgibbon, A. W., and Naidu, D. K. (1998). Calibration, data consistency and model acquisition with a 3-d laser striper. *International Journal of Computer Integrated Manufacturing*, 11(4):293–310.

Wang, X., Cheng, Y., Collins, R., and Hanson, R. (1996). Determining correspondences and rigid motion of 3-d point sets with missing data. In *Proceedings of the IEEE Conference on Computer Vision and Pattern Recognition*, pages 252–257.

Zhang, Z. (1994). Iterative point matching of free-form curves and surfaces. *International Journal of Computer Vision*, 13(2):119–152.

Fig. 1. Cloud-of-points tests: example of registration with missing data (outliers). From left to right: starting position, ICP alignment, RICP alignment.

Fig. 2. RMS error, rotation error and translation error vs standard deviation of Gaussian noise and number of outliers. Cloud-of-points tests. Top row: ICP results. Bottom row: RICP results.

Fig. 3. Calibration jig tests: example of registration with missing data (outliers). From left to right: starting position, ICP alignment, RICP alignment.

Fig. 4. RMS error, rotation error and translation error vs. standard deviation of Gaussian noise and number of outliers. Calibration jig tests. Top row: ICP results. Bottom row: RICP results.

Fig. 5. Basins of attraction. Final RMS (left) and rotation error (right) for ICP (dashed line and circles) and RICP (solid line and crosses) with increasing initial rotation angle.

Fig. 6. A case in which RICP finds the correct registration and ICP does not. From left to right: starting position, ICP alignment, RICP alignment.

Fig. 7. Two range views of a mechanical widget (top row). The registration found by RICP, from two viewpoints (bottom row). All views are subsampled for display.

Fig. 8. Residual histograms for the widget experiment.

Pattern Recognition Letters - Trucco Fusiello Roberto - Figure 1

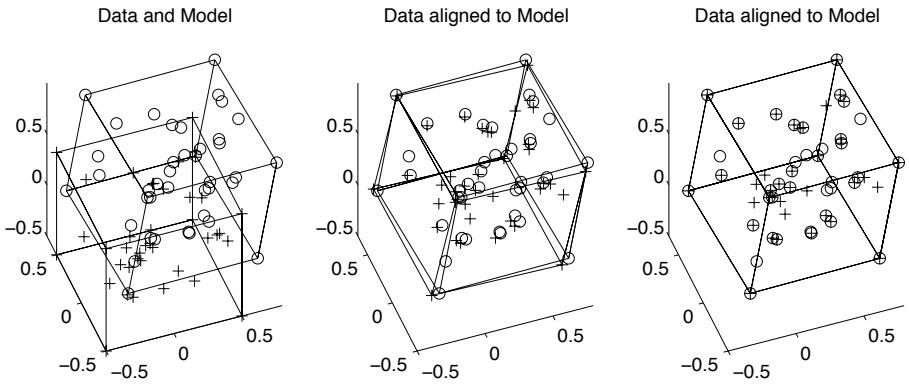

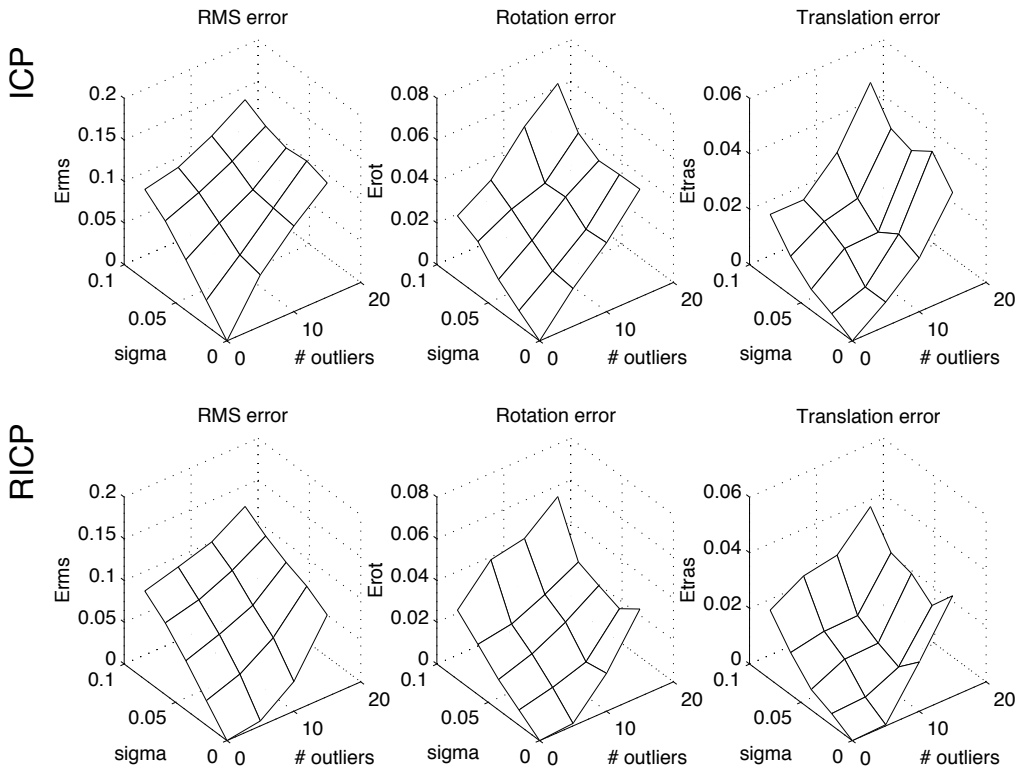
ICP
RMS error
Rotation error
Translation error
Erms
Erot
Etras
sigma
outliers
RICP
RMS error
Rotation error
Translation error
Erms
Erot
Etras
sigma
outliers

Pattern Recognition Letters - Trucco Fusiello Roberto - Figure 3

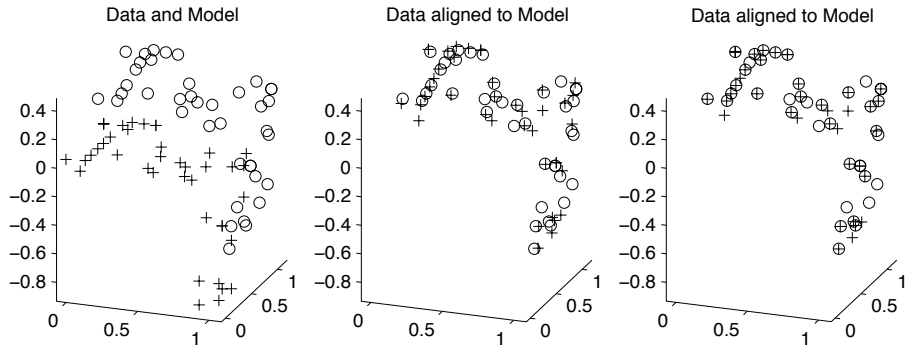

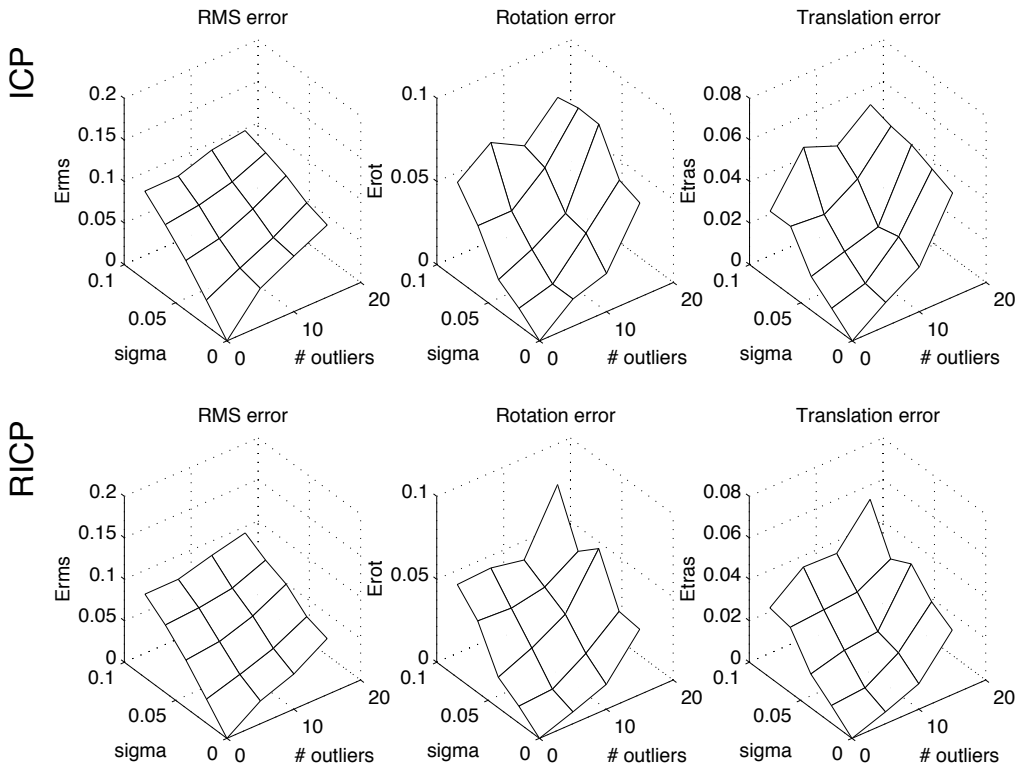
ICP
RICP
RMS error
Rotation error
Translation error
Erms
Erot
Etras
sigma
outliers
0
0.05
0.1
0.15
0.2
0.02
0.04
0.06
0.08
10
20

Pattern Recognition Letters - Trucco Fusiello Roberto - Figure 5

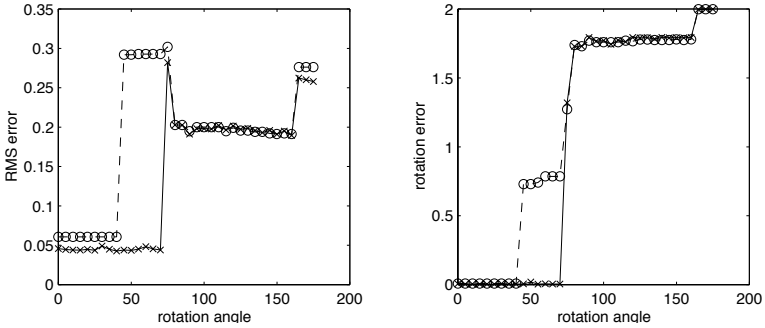

Pattern Recognition Letters - Trucco Fusiello Roberto - Figure 6

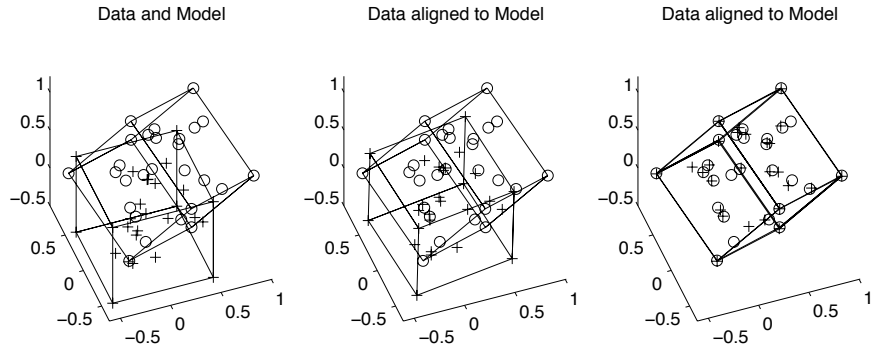

Pattern Recognition Letters - Trucco, Fusiello, Roberto - Figure 7

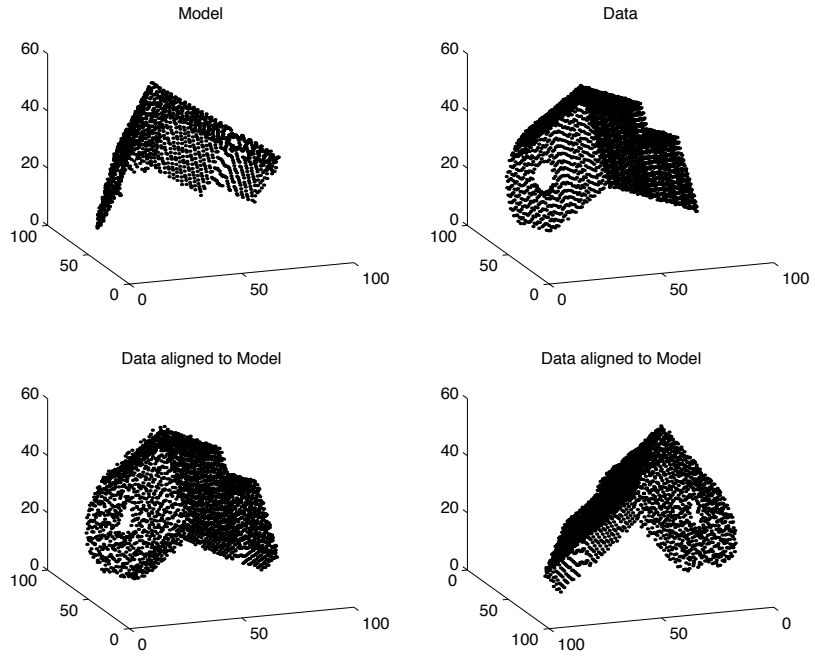

Pattern Recognition Letters - Trucco Fusiello Roberto - Figure 8